



Published in final edited form as:

Nature. ; 481(7380): 209–213. doi:10.1038/nature10697.

Snorkeling Basic Amino Acid Side Chains Regulate Transmembrane Integrin Signalling

Chungho Kim^{1,*}, Thomas Schmidt^{2,*}, Eun-Gyung Cho³, Feng Ye¹, Tobias S. Ulmer^{2,**}, and Mark H. Ginsberg^{1,**}

¹Department of Medicine, University of California-San Diego, La Jolla, CA 92093

²Department of Biochemistry and Molecular Biology, Zilkha Neurogenetic Institute, Keck School of Medicine, University of Southern California, Los Angeles, CA 90033

³Center for Neuroscience, Aging, and Stem Cell Research, Sanford-Burnham Medical Research Institute, La Jolla, CA 92037

Abstract

Side chains of Lys/Arg near transmembrane domain (TMD)^{1–3} membrane-water interfaces can “snorkel” placing their positive charge near negatively-charged phospholipid head groups^{4–6}; however, snorkeling's functional effects are obscure. Integrin β TMDs exhibit such conserved basic amino acids; here we used nuclear magnetic resonance (NMR) spectroscopy^{7, 8} to show that integrin $\beta 3$ (Lys716) helps determine $\beta 3$ TMD topography. The α IIb $\beta 3$ TMD structure suggests that precise $\beta 3$ TMD crossing angles enable the assembly of outer and inner membrane “clasps” (OMC and IMC) that hold the $\alpha\beta$ TMD together to limit transmembrane signalling⁹. Mutation of $\beta 3$ (Lys716) caused dissociation of α IIb $\beta 3$ TMDs and integrin activation. To confirm that altered topography of $\beta 3$ (Lys716) mutants activated α IIb $\beta 3$, we utilized directed evolution of $\beta 3$ (K716A) to identify substitutions restoring default state. Introduction Pro(711) at the midpoint of $\beta 3$ TMD (A711P) increased α IIb $\beta 3$ TMD association and inactivated integrin α IIb $\beta 3$ (A711P,K716A). $\beta 3$ (Pro711) introduced a TMD kink of $30 \pm 1^\circ$ precisely at the OMC/IMC border, thereby decoupling the tilt between these segments. Thus, widely-occurring snorkeling residues in TMDs can help maintain TMD topography and membrane-embedding thereby regulating transmembrane signalling.

Users may view, print, copy, download and text and data-mine the content in such documents, for the purposes of academic research, subject always to the full Conditions of use: http://www.nature.com/authors/editorial_policies/license.html#terms

Correspondence should be addressed to M.H.G. mhginsberg@ucsd.edu or TSU. tulmer@usc.edu.

* and ** denote equal contributions

Mark H. Ginsberg, Dept. of Medicine, University of California-San Diego, La Jolla, CA 92093, Tel: (858) 822-5703 / Fax: (919) 966-1856, mhginsberg@ucsd.edu

Author Contributions: The project was conceived by CK and MHG. All experiments with the exception of the NMR studies were performed by CK. The NMR studies were conducted by TS under the supervision of TSU. EC and FY contributed valuable reagents. MHG and CK wrote the paper which was edited by TS and TSU.

Reprints and permissions information is available at www.nature.com/reprints.

The authors declare no competing financial interest.

Supplementary Information is linked to the online version of the paper at www.nature.com/nature.

Integrins are composed of α and β Type I transmembrane subunits¹⁰; association of the α and β TMDs regulates bidirectional transmembrane signal transduction¹¹. Most metazoan integrin β subunits contain a positively charged Lys or Arg (Fig. 1a) near the inner TMD boundary that precedes an additional hydrophobic patch, termed the ‘membrane proximal region’¹². The membrane proximal region of integrin $\beta 3$ and, in particular, Lys716, is protected from paramagnetic $\text{Mn}^{2+}\text{EDDA}^{2-}$, and is therefore membrane-embedded. This region in other integrin β subunits is also embedded¹³; hence, the membrane proximal domain is the C-terminal limb of a long α -helical TMD that is tilted at an angle of $\sim 25^\circ$, thus enabling the ϵ -amino group of $\beta 3(\text{Lys}716)$ to snorkel near phospholipid head groups⁷.

To assess the role of $\beta 3(\text{Lys}716)$ in TMD topography, we mutated it to a Glu residue and assessed embedding in phospholipid bicelles by measuring protection of the backbone amide protons from the electroneutral paramagnetic $\text{Mn}^{2+}\text{EDDA}^{2-}$ agent^{7, 8}. Lipid embedding on the extracellular side, defined by the protection pattern of Leu694-Val696, was unchanged in $\beta 3(\text{K}716\text{E})$ (Fig. 1b). In contrast, $\beta 3(\text{K}716\text{E})$ reduced protection on the intracellular side by approximately five residues, shifting the membrane border from residue 721 to 716 and decreasing membrane crossing angle. The absence of significant $^{13}\text{C}_\alpha$ chemical shift changes between $\beta 3$ and $\beta 3(\text{K}716\text{E})$ indicated no change in secondary structure as a consequence of the mutation (sFig. 1a). At the level of H^{N} shifts, which are sensitive to surrounding chemical environment, relatively small H^{N} chemical changes between $\beta 3$ and $\beta 3(\text{K}716\text{E})$ indicated limited rearrangements in bicelle structure (Fig. 1c), suggesting that Glu716 still localized within the lipid-water interface. In analogy to the $\text{K}716(\epsilon\text{-NH}_3^+)\text{-lipid}(\text{PO}_4^-)$ snorkeling interaction, glutamate’s $\gamma\text{-COO}^-$ group may engage a POPC lipid’s choline $\text{N}(\text{CH}_3)_3^+$ group or amino NH_3^+ group within the lipid head group region (Fig. 1d). $\beta 3(\text{K}716\text{E})$ TMD-tail was not aggregated (sFig. 1b), indicating that displacement of negatively charged Glu716 from the hydrophobic core shifted Leu(717)-Ile(721) into a more polar environment. Thus, Lys716 substitutions perturb $\beta 3$ TMD membrane embedding and crossing angle.

Disruption of the interaction between integrin α and β TMDs leads to allosteric rearrangements that result in increased ligand-binding affinity of the extracellular domain (integrin activation)^{10, 11, 14} and activation of cytosolic signalling pathways¹⁵. A stable $\alpha\beta$ TMD association, which is crucial in the regulation of and physiological functions of integrins, requires the simultaneous formation of two discrete assemblies, an inner and outer membrane clasp (IMC and OMC), respectively (Fig. 1e)⁹. Since the $\beta 3$ TMD forms a continuous α -helix, its crossing angle appears critical for the simultaneous assembly of these clasps⁹. To examine the effect of $\beta 3(\text{Lys}716)$ mutations on the $\alpha\text{IIb}\beta 3$ TMD association in mammalian cell membranes, we used a mini-integrin affinity capture assay¹⁶ and chemical cross-linking. The latter experiments showed that the $\alpha\text{IIb}\beta 3$ TMD interaction is primarily a 1:1 heterodimer (sFig.2). For the capture assay, an αIIb mini-integrin bait containing the TMD and cytoplasmic tail of αIIb (Fig. 2a) joined to a C-terminal tandem affinity purification (TAP) tag¹⁶ for rapid efficient purification was expressed with preys comprising the extracellular domain of the Tac (IL-2 receptor α) joined to the TMD and tail of $\beta 3$ or $\beta 3$ bearing Lys716 substitutions (Fig. 2a). When the cells were lysed and baits were captured using calmodulin beads, we found that the αIIb bait captured the $\beta 3$ prey, as expected; however, neutral (Ala), polar (Cys, Ser), Acidic (Glu), or hydrophobic (Leu) substitutions at

$\beta 3(\text{Lys}716)$ blocked the $\alpha\text{IIb}\beta 3$ TMD association. In contrast, a basic amino acid substitution (Arg) did not disrupt the association consistent with the idea that a snorkeling residue in this position is required to the formation of the $\alpha\text{IIb}\beta 3$ TMD complex. To examine the potential effects of $\beta 3(\text{Lys}716)$ mutations on transmembrane signalling, we assayed their effects on the affinity state of integrin $\alpha\text{IIb}\beta 3$ by measuring binding to activation-specific $\alpha\text{IIb}\beta 3$ antibody (PAC1)¹⁷ as in Fig. 2b. The results precisely correlated with the effects on $\alpha\beta$ TMD interaction; all substitutions with the exception of Arg led to spontaneous integrin activation (Fig. 2c). The importance of this highly conserved Lys seems general because mutation of the paralogous residue in integrin $\beta 1\text{A}$ (K732E) activated integrin $\alpha 5\beta 1$ (sFig. 3a–d) and inhibited the association of the $\beta 1$ TMD with either the $\alpha 5$ or αV TMD (sFig. 3e). Thus, loss of a conserved basic residue in integrin β TMDs leads to disruption of the α - β TMD interaction and spontaneous transmembrane signalling.

The findings that $\beta 3(\text{Lys}716)$ substitutions that prohibit snorkeling alter TMD embedding, that such mutations dissociate the $\alpha\text{IIb}\beta 3$ TMD complex and activate integrins, and the predicted importance of the crossing angle in maintenance of the two clasps that stabilize the $\alpha\beta$ TMD association support the idea that the snorkeling Lys controls transmembrane signalling by specifying the embedding and crossing angle of the $\beta 3$ TMD. Nevertheless, Rosetta modeling with sparse restraints provided by Cystine cross-linking predicted seven clusters of integrin $\alpha\text{IIb}\beta 3$ TMD structures¹⁸, some of which resembled the calculated NMR structure⁹. The Rosetta structures suggested that $\beta 3(\text{Lys}716)$ can form hydrogen bonds with αIIb backbone carbonyl groups of Phe992 and Phe993, thereby stabilizing the α - β interaction¹⁸ and the same paper reported that mutations at $\beta 3(\text{Lys}716)$ resulted in integrin activation¹⁸, a result we confirmed above. However, NMR-based structural restraints⁹ preclude $\beta 3(\text{Lys}716/\epsilon\text{-NH}_3^+)$ - $\alpha\text{IIb}(\text{Phe}993/\text{CO})$ interactions (sFig. 4). Furthermore, the embedding of the isolated $\beta 3$ TMD was similar to that observed in the $\alpha\text{IIb}\beta 3$ complex⁹ and, as shown above, loss of the snorkeling $\beta 3(\text{Lys}716)$ alters $\beta 3$ TMD embedding. We therefore sought a positive experimental confirmation that the effects of $\beta 3(\text{Lys}716)$ mutations on $\alpha\text{IIb}\beta 3$ TMD association and on integrin activation could be ascribed to changes in the $\beta 3$ membrane topography.

If $\beta 3(\text{Lys}716)$ mutations changed topography to prevent the simultaneous formation of the IMC and OMC, thereby leading to integrin activation, we reasoned that compensating mutations within the $\beta 3$ TMD might exist that would correct the crossing angle. Conversely, if $\beta 3(\text{Lys}716)$ formed hydrogen bonds with the αIIb , then a compensating mutation might introduce additional basic residues that could form such bonds.

We used random mutagenesis in a window of 5 residues N-terminal and 10 residues C-terminal to the $\beta 3(\text{K}716)$ substitution (Fig. 3a and sFig. 6a) to identify mutations that would complement the activating effects. We chose $\beta 3(\text{K}716\text{A})$ as the activating mutation; its effects may be less profound than $\beta 3(\text{K}716\text{E})$, thus favoring the discovery of weakly compensating mutations. Lentivirus particles carry two genomes²⁰, making it possible that a single particle might encode two mutants. To test this possibility, we transfected packaging cells with a mixture of lentiviral plasmids encoding integrin $\beta 3$ and $\beta 3(\text{K}716\text{A})$. When CHO cells bearing integrin αIIb were infected with the resulting viruses, we found only populations containing either fully active or fully inactive $\alpha\text{IIb}\beta 3$, with no intermediate

phenotype (sFig. 5). Thus, the packaging cells incorporated two copies of identical genomes into each viral particle. We performed PCR using a primer that was synthesized with 9% contamination of incorrect nucleotides in the randomized windows. The contamination level was predicted by computer simulation to cover most single amino acid changes within the window (sFig. 6b and sTable 1). We ligated the PCR fragments containing random mutations into a lentiviral vector encoding full-length integrin $\beta 3$, to create a randomized $\beta 3$ cDNA library (Fig. 3b).

CHO/ α IIB cells were infected with the mutant $\beta 3$ lentiviral particles and the infected cells were analyzed for integrin expression (D57 antibody binding) and activation (PAC1 antibody binding) by using flow cytometry (Fig. 3b). In contrast to the $\beta 3$ (K716A)-infected cells, cells infected with the mutant $\beta 3$ library exhibited a population of cells that expressed inactive α IIB $\beta 3$ (R3 region in Fig. 3c). To identify those mutations, we collected ~7,000 cells in the R3 region and purified genomic DNAs from those cells and used PCR to isolate the region of integrin $\beta 3$ containing the mutagenized window (Fig. 3b). Sequencing of the bulk product revealed that a $\beta 3$ (A711P) mutation and stop codons at residue 724 and 725 were found in the mutagenized window (Fig. 3d). We performed NheI and BamHI digestion to isolate individual fragments containing the mutations and, after ligation into wild type integrin $\beta 3$, confirmed the compensating effect of the mutations by transient transfection into cells expressing wild-type integrin α IIB and measuring PAC1 binding (sFig. 7). The clones that showed a compensating effect were sequenced and fell into 3 major groups (Fig. 3e): clones containing Pro substitutions at Ala711 position (group 1), stop codons at Arg724 or Lys725 positions (group 2), or a neutral residue substitution at Glu726 position (group 3).

The only compensating mutation consistently observed in the TMD was $\beta 3$ (A711P) (Group 1 in Fig. 3e). This represents an integrin TMD point mutation that inhibits transmembrane signaling. This residue is inaccessible to talin or other cytoplasmic proteins and is unlikely to provide a direct interaction with α IIB since it is not in the α - β TMD binding interface⁹. We confirmed that $\beta 3$ (A711P) compensates both $\beta 3$ (K716A) and $\beta 3$ (K716E) mutations with respect to integrin activation. (Fig. 4a, sFig. 8b). In addition, $\beta 3$ (A711P) increased interaction of the $\beta 3$ (K716A) TMD with that of α IIB (Fig. 4b). In contrast, the two other groups of compensating mutations were in the $\beta 3$ cytoplasmic domain. The truncated $\beta 3$ caused by $\beta 3$ (724X or 725X) (group 2) deletes the talin binding site in the $\beta 3$ tail²¹. Furthermore, $\beta 3$ Glu726 can contribute to talin binding via electrostatic interactions with Lys317 and Lys364 in talin²². Thus, we suspected that talin binding might amplify the activating effect of $\beta 3$ (K716A); to test this idea we examined its effects in conjunction with $\beta 3$ (Y747A) a mutation that disrupts talin binding¹⁵. Indeed the α IIB $\beta 3$ (K716A, Y747A) mutant was less active than α IIB $\beta 3$ (K716A) (sFig. 8a). Thus, the only consistent TMD mutation that compensated for $\beta 3$ (Lys716) substitutions was the introduction of a Pro at position 711.

The structure of the $\beta 3$ (A711P, K716A) TMD peptide embedded in phospholipid bicelles was determined. In accordance with the capacity of Pro to introduce kinks in TM helices²³, A711P induced a $30 \pm 1^\circ$ kink between preceding and succeeding helical segments (Fig. 4c) caused by the disruption of helix-stabilizing hydrogen bonds between Ile707 and the proline residue and also between Gly707 and Leu712 (sFig. 9). This kink precisely separated the α -

helical segments of $\beta 3$ that constitute the inner and outer clasps. Moreover, A711P introduced a tilt between these elements that is independent of the overall membrane $\beta 3$ TMD crossing angle. Thus, even if the tilt angle of the inner helix is perturbed, this kink can aid the formation of both inner and outer membrane clasps⁹ to stabilize the $\alpha\beta$ dimer. To verify that both clasps still partake in maintaining the inactive state of the integrin, mutations that disrupted either clasp were examined. The OMC involves packing interactions of αIIb (Gly972 and Gly976) and $\beta 3$ (Gly708)^{9, 24}. αIIb (G972,976A) substitutions that disrupt the OMC overcame the compensating effect of $\beta 3$ A711P in both of K716A and K716E background (Fig. 4d). Similarly, the αIIb (R995D) mutation or αIIb (GFFKR) deletion, which disrupt the IMC, also overcame compensation (Fig. 4d). Thus, the kink introduced by $\beta 3$ (A711P) allows the formation of the two membrane clasps required to stabilize the integrin in the off state (Fig. 4e).

In sum, we demonstrated that the loss of a snorkeling residue in integrin β TMDs can change membrane embedding and, thus, membrane-crossing angle, providing direct evidence that snorkeling can specify the topography of TMDs. Furthermore, we showed that the snorkeling can affect transmembrane signalling by altering the stability of interactions between integrin TMDs. We developed an efficient random lentiviral mutagenesis screening method, which was used to discover that a Pro-induced helix kink led to the stabilization of integrin α and β TMDs interaction by facilitating the formation of the inner and outer membrane clasps. Thus, the long-appreciated snorkeling of basic residues in TMDs¹⁻³ can play an important role in their topography and lateral association and therefore in signal transduction.

Methods summary

NMR spectroscopy

Peptides encompassing human integrin $\beta 3$ (P685-F727), either wild type or K716E mutant, were produced enriched in ^{15}N or $^2\text{H}/^{13}\text{C}/^{15}\text{N}$ isotopes as described previously⁷. Defined amounts of freeze-dried peptide were reconstituted in 25 mM HEPES•NaOH, pH 7.4, 6 % D_2O , 0.02 % w/v NaN_3 solution containing 200 mM 1,2-Dihexanoyl-*sn*-Glycero-3-Phosphocholine (DHPC), 40 mM 1-Palmitoyl-2-Oleoyl-*sn*-Glycero-3-Phosphocholine (POPC) and 20 mM 1-Palmitoyl-2-Oleoyl-*sn*-Glycero-3-[Phospho-L-Serine] (Avanti Polar Lipids, Inc.). 2D TROSY H-N experiments were recorded in the absence and presence of 1 mM Mn^{2+} /EDDA²⁻ using peptide concentrations of 0.2 mM⁸. K716E assignment was transferred from the wild type using HNCA experiments.

Random $\beta 3$ library construction

Integrin $\beta 3$ (K716A) cDNA was mutated to remove BamHI site and introduce NheI site with silent mutations. The cDNA was cloned into lentiviral vector which is modified from pRRLSIN.cPPT.PGK-IRES-GFP.WPRE (Addgene) to have BamHI site and BGH reverse primer binding site between PGK promoter and IRES-GFP. The region between NheI and BamHI site were cut out, and replaced with NheI and BamHI restricted mutagenized PCR products by ligation. The mutagenized PCR products were generated using BGH reverse primer and mutagenized forward primer (sFig. 6a). A total ~310,000 E.coli colonies on

plates from the ligation reaction were harvested and pooled. Plasmids from those cells were purified to make the mutagenized $\beta 3$ cDNA library.

Methods

Plasmids, antibody, and cell lines

α IIBTM-TAP, Tac- $\beta 3$ TM constructs¹⁶, and lentiviral cloning vector (pRRLSIN.cPPT.PGK-IRES-GFP.WPRE)²⁶ were described previously. Site specific mutagenesis was performed using the Quick change site-directed mutagenesis kit (Stratagen). Anti-Tac N19 (Santa Cruz Biotechnology), anti-Flag M2 (Sigma-aldrich), and anti-HA 16B12 (Covance) antibodies were obtained commercially. Mouse monoclonal antibody specific for the human integrin α IIB $\beta 3$ (D57) and activation-specific anti α IIB $\beta 3$ antibody (PAC1) have been described previously¹³. Chinese hamster ovary (CHO) cell were maintained as described previously¹³. CHO/ α IIB cells were prepared by infecting CHO cells with lentiviral particle containing integrin α IIB. Lipofectamine and Lipofectamine Plus reagents (Invitrogen) were used according to the manufacturer's recommendation for transient transfections.

Affinity capture

α IIBTM-TAP were co-transfected into CHO cells with Tac- $\beta 3$ TM bearing various mutations, and their affinities were analyzed as described previously¹⁶.

Flow cytometry

PAC1 binding assay were performed as described^{16, 27}. In brief, one day after transfection, suspended cells were incubated with D57 in combination with PAC1, followed by staining with allophycocyanin (APC)-conjugated anti-mouse IgG and with R-phycoerythrin (PE)-conjugated anti-mouse IgM. Five min prior to analysis, propidium iodide (PI) was added, and PI-negative cells were analyzed on FACSCalibur (BD Biosciences). The data were imported into MATLAB R2009a software, and the geometric means of PAC1 binding in cells expressing specified levels of α IIB $\beta 3$ expression were calculated. Those mean values were indicated in the dot plots as larger red dots, and also used for the line graphs.

NMR spectroscopy

Peptide encompassing human integrin $\beta 3$ (P685-F727), including $\beta 3$ (C687S), was produced enriched in ¹⁵N or ²H/¹³C/¹⁵N isotopes as described previously⁷. K716E substitution was introduced using QuikChange mutagenesis (Stratagene, Inc.) and the peptide was produced analogously to wild-type $\beta 3$. Defined amounts of freeze-dried peptide was reconstituted in 25 mM HEPES-NaOH, pH 7.4, 6% D₂O, 0.02% w/v NaN₃ solution containing 200 mM 1,2-Dihexanoyl-*sn*-Glycero-3-Phosphocholine (DHPC), 40 mM 1-Palmitoyl-2-Oleoyl-*sn*-Glycero-3-Phosphocholine (POPC) and 20 mM 1-Palmitoyl-2-Oleoyl-*sn*-Glycero-3-[Phospho-L-Serine] (Avanti Polar Lipids, Inc.). 2D TROSY H-N experiments were recorded in the absence and presence of 1 mM Mn²⁺EDDA²⁻ using peptide concentrations of 0.2 mM⁸. K716E assignment was transferred from the wild type using HNCA experiments. The structure of $\beta 3$ (A711P, K716A) was determined in 350 mM DHPC, 105 POPC as described previously for the corresponding wild-type peptide⁷. Structural statistics and spectral quality

are summarized in supplemental Tables 2–3 and sFig. 10). All NMR experiments were conducted on a cryoprobe-equipped Bruker Avance 700 spectrometer at 35 °C.

Random $\beta 3$ library construction

Integrin $\beta 3$ (K716A) cDNA was mutated to remove BamHI site and introduce NheI site with silent mutations. The cDNA was cloned into lentiviral vector which is modified from pRRLSIN.cPPT.PGK- IRES-GFP.WPRE (Addgene) to have BamHI site and BGH reverse primer binding site between PGK promoter and IRES-GFP. The region between NheI and BamHI site (corresponding to the integrin $\beta 3$ region containing C-terminal TMD and full cytoplasmic tail, sFig. 6a) were cut out, and replaced with NheI and BamHI restricted mutagenized PCR products by ligation. The mutagenized PCR products were generated using BGH reverse primer and mutagenized forward primer (5'-cattgggctagccGCCCTGCTCATCTGGgcaCTCCTCATCACCATCCACGACCGAAAAGAAttgctaatttg aggaag-3', where capital letter represents the position containing 9% of contaminating nucleotide, sFig. 6a). A total ~310,000 *E.coli* colonies on plates from the ligation reaction were harvested and pooled. Plasmids from those cells were purified to make the mutagenized $\beta 3$ cDNA library.

Supplementary Material

Refer to Web version on PubMed Central for supplementary material.

Acknowledgments

Supported by grants from the National Institutes of Health of the USA. TSU acknowledges support from the National Institutes of Health (HL089726) and MHG was supported by HL078784, HL57900, and AR27214. CK is a recipient of postdoctoral fellowship from American Institute for Cancer Research.

References

1. Killian JA, von Heijne G. How proteins adapt to a membrane-water interface. *Trends Biochem Sci.* 2000; 25:429–34. [PubMed: 10973056]
2. von Heijne G. Membrane proteins: from sequence to structure. *Annu Rev Biophys Biomol Struct.* 1994; 23:167–92. [PubMed: 7919780]
3. Sipos L, von Heijne G. Predicting the topology of eukaryotic membrane proteins. *Eur J Biochem.* 1993; 213:1333–40. [PubMed: 8099327]
4. Krishnakumar SS, London E. The control of transmembrane helix transverse position in membranes by hydrophilic residues. *J Mol Biol.* 2007; 374:1251–69. [PubMed: 17997412]
5. Strandberg E, Killian JA. Snorkeling of lysine side chains in transmembrane helices: how easy can it get? *FEBS Lett.* 2003; 544:69–73. [PubMed: 12782292]
6. Strandberg E, et al. Lipid dependence of membrane anchoring properties and snorkeling behavior of aromatic and charged residues in transmembrane peptides. *Biochemistry.* 2002; 41:7190–8. [PubMed: 12044149]
7. Lau TL, Partridge AW, Ginsberg MH, Ulmer TS. Structure of the integrin beta3 transmembrane segment in phospholipid bicelles and detergent micelles. *Biochemistry.* 2008; 47:4008–16. [PubMed: 18321071]
8. Lau TL, Dua V, Ulmer TS. Structure of the integrin alphaIIb transmembrane segment. *J Biol Chem.* 2008; 283:16162–8. [PubMed: 18417472]

9. Lau TL, Kim C, Ginsberg MH, Ulmer TS. The structure of the integrin alphaIIb beta3 transmembrane complex explains integrin transmembrane signalling. *Embo J*. 2009; 28:1351–61. [PubMed: 19279667]
10. Arnaout MA, Mahalingam B, Xiong JP. Integrin structure, allostery, and bidirectional signaling. *Annu Rev Cell Dev Biol*. 2005; 21:381–410. [PubMed: 16212500]
11. Shattil SJ, Kim C, Ginsberg MH. The final steps of integrin activation: the end game. *Nat Rev Mol Cell Biol*. 2010; 11:288–300. [PubMed: 20308986]
12. Ginsberg MH, Partridge A, Shattil SJ. Integrin regulation. *Curr Opin Cell Biol*. 2005; 17:509–16. [PubMed: 16099636]
13. Stefansson A, Armulik A, Nilsson I, von Heijne G, Johansson S. Determination of N- and C-terminal borders of the transmembrane domain of integrin subunits. *J Biol Chem*. 2004; 279:21200–5. [PubMed: 15016834]
14. Hynes RO. Integrins: bidirectional, allosteric signaling machines. *Cell*. 2002; 110:673–87. [PubMed: 12297042]
15. Zhu J, et al. Requirement of alpha and beta subunit transmembrane helix separation for integrin outside-in signaling. *Blood*. 2007; 110:2475–83. [PubMed: 17615290]
16. Kim C, Lau TL, Ulmer TS, Ginsberg MH. Interactions of platelet integrin alphaIIb and beta3 transmembrane domains in mammalian cell membranes and their role in integrin activation. *Blood*. 2009; 113:4747–53. [PubMed: 19218549]
17. Shattil SJ, Hoxie JA, Cunningham M, Brass LF. Changes in the platelet membrane glycoprotein IIb/IIIa complex during platelet activation. *J Biol Chem*. 1985; 260:11107–14. [PubMed: 2411729]
18. Zhu J, et al. The structure of a receptor with two associating transmembrane domains on the cell surface: integrin alphaIIb beta3. *Mol Cell*. 2009; 34:234–49. [PubMed: 19394300]
19. Tugarinov V, Kay LE. Ile, Leu, and Val methyl assignments of the 723-residue malate synthase G using a new labeling strategy and novel NMR methods. *J Am Chem Soc*. 2003; 125:13868–78. [PubMed: 14599227]
20. Frankel AD, Young JA. HIV-1: fifteen proteins and an RNA. *Annu Rev Biochem*. 1998; 67:1–25. [PubMed: 9759480]
21. Tadokoro S, et al. Talin binding to integrin beta tails: a final common step in integrin activation. *Science*. 2003; 302:103–6. [PubMed: 14526080]
22. Anthis NJ, et al. The structure of an integrin/talin complex reveals the basis of inside-out signal transduction. *Embo J*. 2009; 28:3623–32. [PubMed: 19798053]
23. Senes A, Engel DE, DeGrado WF. Folding of helical membrane proteins: the role of polar, GxxxG-like and proline motifs. *Curr Opin Struct Biol*. 2004; 14:465–79. [PubMed: 15313242]
24. Berger BW, et al. Consensus motif for integrin transmembrane helix association. *Proc Natl Acad Sci U S A*. 2010; 107:703–8. [PubMed: 20080739]
25. Rosenbaum DM, Rasmussen SG, Kobilka BK. The structure and function of G-protein-coupled receptors. *Nature*. 2009; 459:356–63. [PubMed: 19458711]
26. Ye F, et al. Recreation of the terminal events in physiological integrin activation. *J Cell Biol*. 2010; 188:157–73. [PubMed: 20048261]
27. Han J, et al. Reconstructing and deconstructing agonist-induced activation of integrin alphaIIb beta3. *Curr Biol*. 2006; 16:1796–806. [PubMed: 16979556]

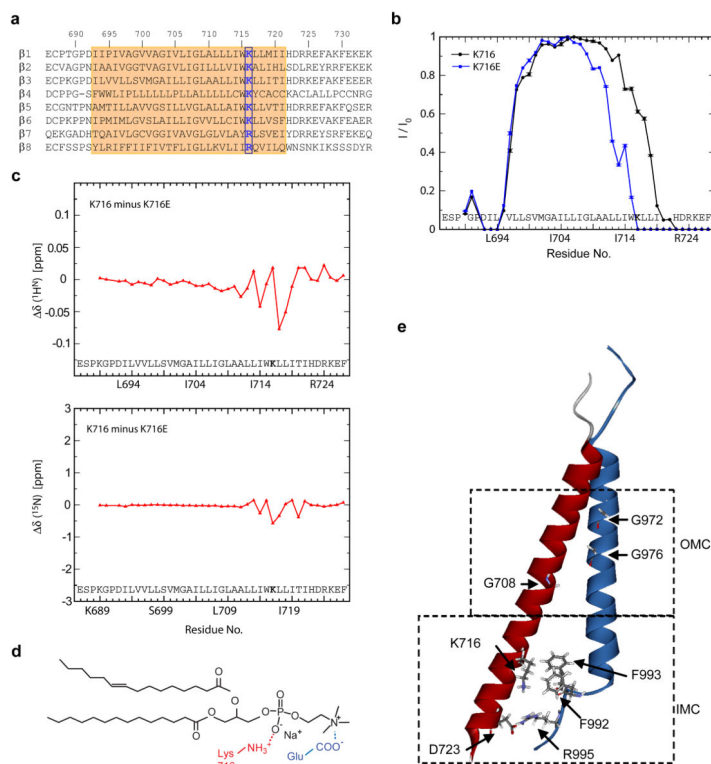


Figure 1. Loss of snorkeling lysine changes lipid embedding of $\beta 3$ TMD

a, Sequence alignment of TMD regions of integrin β subunits indicated with $\beta 3$ numbering. Transmembrane domains are highlighted in orange. Conserved positive charged amino acids at position 716 (of $\beta 3$) are bolded and boxed with blue line. **b**, Mutation of $\beta 3$ (Lys716) changes TMD membrane embedding. The TROSY H-N cross-peak signal intensity of a residue in the presence and absence of 1 mM $Mn^{2+}EDDA^{2-}$ in the aqueous phase, I/I_0 , was measured to quantitatively express protection from the paramagnetic reagent. Experiments were performed in duplicates using independently prepared samples and quote the standard error between datasets. **c**, Chemical shift changes of K716E relative to the wild type. **d**, The predicted interaction of Lys716 side chain ϵ - NH_3^+ with a lipid's PO_4^- group (red) and the interaction of glutamate's γ - COO^- with a POPS lipid's amino NH_3^+ group (blue) are illustrated. **e**, NMR structure of integrin $\alpha IIb\beta 3$ TMD (PDB ID 2K9J). Side chains of residues essential to forming the OMC (Gly972, G976 in αIIb , and Gly708 in $\beta 3$) and the IMC (Phe992, Phe993, Arg995 in αIIb , Asp723 in $\beta 3$) are indicated.

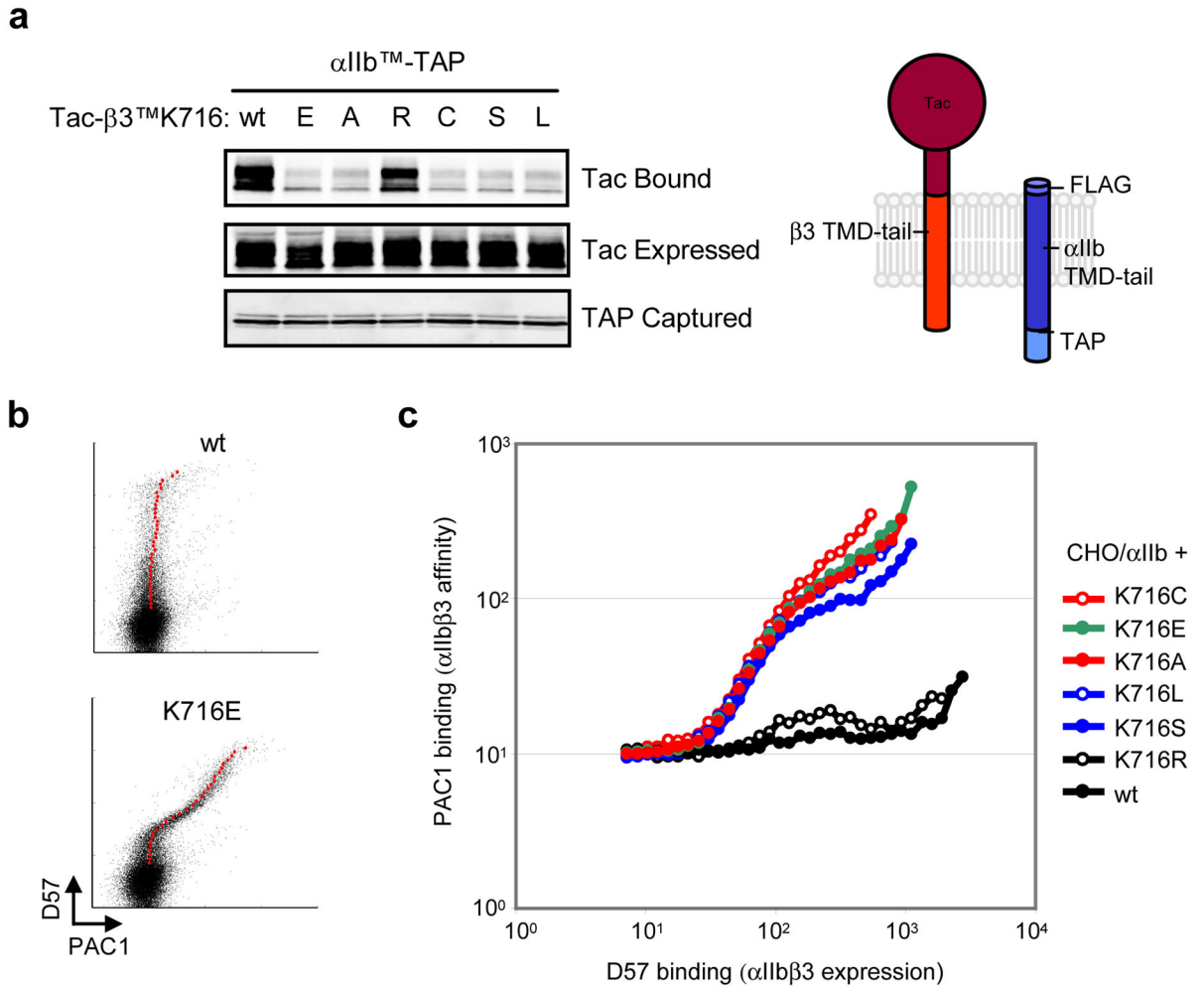


Figure 2. Mutations in the snorkeling lysine induce integrin activation and disrupt α - β TMD interaction

a, Mutations of $\beta 3$ (Lys716) disrupt the α IIb $\beta 3$ TMD interaction. CHO cells were co-transfected with α IIb TMD-tail construct fused with C-terminal TAP tag, α IIbTM-TAP, and $\beta 3$ TMD-tail constructs fused with N-terminal Tac extracellular domain, Tac- $\beta 3^{\text{TM}}$, bearing various mutations at $\beta 3$ (K716) as indicated. α IIbTM-TAP proteins were isolated and associated Tac- $\beta 3^{\text{TM}}$ was detected by western blotting (upper panel). Expressed Tac- $\beta 3^{\text{TM}}$ proteins (middle panel) and captured α IIbTM-TAP proteins (bottom panel) are also shown. **b**, $\beta 3$ (K716E) activates integrin α IIb $\beta 3$. CHO cells stably expressing integrin α IIb (CHO/ α IIb) were transiently transfected with wild type (wt) integrin $\beta 3$ or $\beta 3$ (K716E). 18 hour later, surface expression (D57 binding) and affinity of α IIb $\beta 3$ (PAC1 binding) were analyzed. Geometric means of PAC1 binding in cells expressing different quantities of α IIb $\beta 3$ were plotted as larger red dots. **c**, Multiple $\beta 3$ (K716) mutations activate integrin α IIb $\beta 3$. CHO/ α IIb cells were transfected with integrin $\beta 3$ bearing different mutations in the K716 residue as indicated. The geometric means of PAC1 binding to those CHO/ α IIb cells were plotted against D57 binding.

neutral residue at E726 position (group 3), and spontaneous mutations that did not fall within the target window (group 4).

Author Manuscript

Author Manuscript

Author Manuscript

Author Manuscript

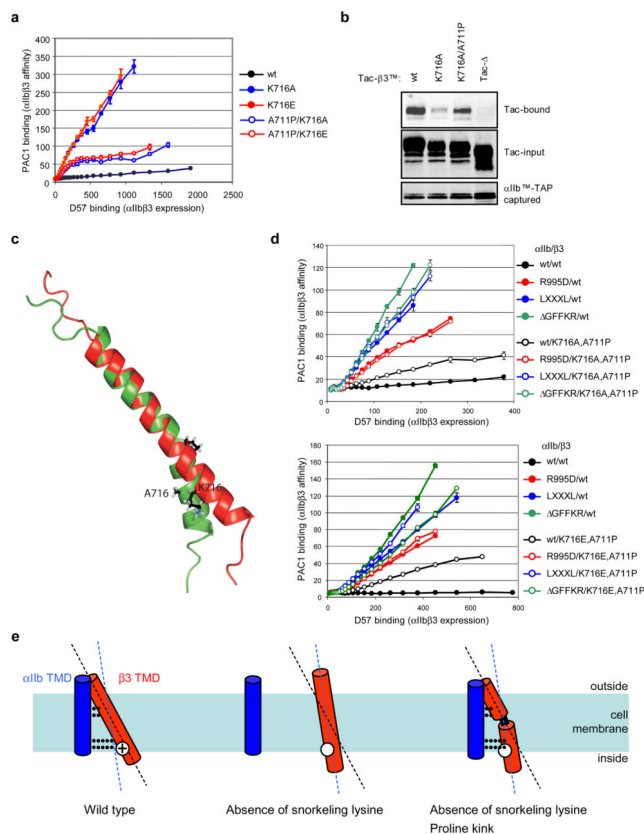


Figure 4. Proline introduced in the TMD forms a flexible kink that stabilizes the α IIb β 3(K716A) TMD interaction and reduces integrin activation

a, β 3(A711P) complements β 3(Lys716) mutations in integrin activation. CHO/ α IIb cells were transiently transfected with various integrin β 3 constructs as indicated, and their binding to PAC1 and D57 was analyzed as described above. Error bars indicate standard errors of the mean (n=3). **b**, β 3(A711P) stabilizes the TMD interactions of α IIb β 3(K716A). CHO cells were co-transfected with α IIbTM-TAP constructs and wild type, or mutant Tac- β 3TM constructs as indicated, and the interaction between those integrin TMDs were analyzed as previously reported¹⁶. **c**, Structure of the β 3(K716A, A711P) TMD. Structure of the bicelle-embedded integrin β 3(A711P, K716A) TMD segment (shown in green, PDB ID 2L91) in comparison to the wild-type β 3 TMD structure (shown in red)⁷. To illustrate the proline-induced kink, the structures were superimposed on the backbone heavy atom coordinates of Ile693-Leu709. Average structures are shown. **d**, The inactive state of α IIb β 3(A711P, K716A/E) requires formation of both IMC and OMC. α IIb mutations that disrupt either the OMC (α IIb G972L, G976L) (LXXXL) or IMC (α IIbR995D or α IIb(G⁹⁹¹FFKR) reactivate the α IIb β 3(K716A, A711P) integrin (upper panel) or α IIb β 3(K716E, A711P) integrin (lower panel). Error bars indicate standard errors (n=3). **e**, Mechanism of proline-mediated compensation of snorkeling mutations. Snorkeling of positive charged residue fixes the crossing angle of β 3 TMD (left). Loss of snorkeling changes the crossing angle and preventing simultaneous formation of IMC and OMC,

thereby disrupting TMD interaction (middle). The Proline-induced kink restores the angle of N-terminal half of the helix (right), enabling reformation of both clasps.

Author Manuscript

Author Manuscript

Author Manuscript

Author Manuscript